Supporting information for

Histone ADP-ribosylation promotes resistance to PARP inhibitors by facilitating PARP1 release from DNA lesions

Siham Zentout[1], Victor Imburchia[1], Catherine Chapuis[1], Lena Duma[2], Kira Schützenhofer[2], Evgeniia Prokhorova[2], Ivan Ahel[2], Rebecca Smith[1,2,*] and Sébastien Huet[1,*]

1 Univ Rennes, CNRS, IGDR (Institut de génétique et développement de Rennes) - UMR 6290, BIOSIT – UMS3480, F- 35000 Rennes, France
2 Sir William Dunn School of Pathology, University of Oxford, South Parks Road, Oxford, OX1 3RE, UK.

*Correspondence to: R.S. (rebecca.smith@path.ox.ac.uk) or S.H. (sebastien.huet@univ-rennes.fr)

This PDF file includes:

Figures S1 to S4
Tables S1 and S2

SUPPLEMENTARY FIGURE LEGENDS

Supplementary figure 1. Heteromodification contributes to the mobilization of PARP1 from the DNA lesions. (A) Representative images of U2OS cells bearing LacO repeats and co-expressing a mCherry-tagged fusion between the LacI and the macrodomain of macroH2A1.1 and GFP tagged PARP1 WT or PARP1 E988K. Images were taken prior to damage and 50 s post irradiation with a pulsed 800 nm laser. Insets pseudocolored according to the look-up table displayed below show magnification of the LacO array. Scale bar, 5 μm. **(B)** Quantification of the PARP1 accumulation at the LacO array from the images shown in A. **(C)** Recruitment kinetics of the GFP tagged PARP1 S499/507/519A E988K (PARP1 3SA-EK) mutant after DNA damage by 405 nm laser irradiation, in PARP1 KO co-expressing or not mCherry tagged PARP1 WT. **(D)** Recruitment kinetics of GFP tagged PARP1 E988K after DNA damage by 405 nm laser irradiation, in PARP1 KO co-expressing or not mCherry tagged PARP1 3SA.

Supplementary figure 2. Impact of PARGi treatment on the nuclear dynamics of PARP1. (A) Normalized FCS correlation curve obtained for GFP tagged PARP1 WT expressed in ARH3 KO cells in the absence of PARGi treatment. The experimental curve (black line) is fitted with an effective-diffusion model (blue line). **(B)** Residence times within the focal volume estimated from the fit of the autocorrelation curves obtained for GFP tagged PARP1 WT expressed in WT cells treated or not with 20µM of the PARGi PDD00017273 for 48h.

Supplementary figure 3. HPF1 dependent histone ADP-ribosylation promotes PARP1 release from DNA breaks. (A) Immunoblot of whole-cell extract from U2OS WT, ARH3 KO, PARP1 KO and PARP1/ARH3 KO cells. The blot was stained with a PARP1 and an ARH3 antibody. H3 staining was used as loading control. **(B-D)** Mean nuclear intensities of mCherry-tagged fusion proteins as indicated. **(E)** Immunoblot of whole-cell extract from U2OS WT, ARH3 KO, HPF1 KO, and HPF1/ARH3 KO cells. The blot was stained with a HPF1 and an ARH3 antibody. PARP1 staining was used as loading control. **(F-H)** Recruitment kinetics (F), dissipation times (G) and mean nuclear intensities in the mCherry channel (H) for GFP tagged PARP1 chromobody after DNA damage by 405 nm laser irradiation, in HPF1/ARH3 KO co-expressing mCherry tagged ARH3 WT or LANA-ARH3 WT. **(I)** Immunoblot of ARH3 KO cells, untransfected, or expressing either GFP tagged ARH3 WT, ARH3 D77/78N (DD), LANA-ARH3 WT LANA-ARH3 D77/78N, H2B-ARH3 WT or H2B-ARH3 D77/78N, treated or not with H_2O_2. The blot was stained with a pan-ADPr and an ARH3 antibody. H3 staining was used as loading control. **(J)** Representative images of UO2S cells bearing LacO repeats and co-expressing a mCherry tagged fusion between the LacI and the macrodomain of macroH2A1.1, PARP1 WT fused to Halotag stained with JF648 and LANA-ARH3 WT or D77/78N tagged with GFP. Images were taken prior to damage and 50 s post 405 nm laser irradiation. Insets pseudocolored according to the look-up table displayed below, show magnification of the LacO array. **(K)** Quantification of PARP1 accumulation at the LacO array from the images shown in I. **(L-N)** Recruitment kinetics (L) dissipation times (M) and mean nuclear intensities in the mCherry channel (N) for GFP tagged PARP1 WT after DNA damage by 405 nm laser irradiation, in PARP1/ARH3 KO co-expressing mCherry tagged ARH3 WT or H2B-ARH3 WT. **(O-Q)** Recruitment kinetics (O), dissipation times (P) and mean nuclear intensities in the mCherry channel (Q) for GFP tagged PARP1 WT after DNA damage by 405 nm laser irradiation, in PARP1/ARH3 KO co-expressing mCherry tagged H2B-ARH3 WT or H2B-ARH3 D77/78N.

Supplementary figure 4. Histone ADP-ribosylation underlies resistance to the PARP inhibitor Olaparib. Immunoblot of whole-cell extract from U2OS WT or ARH3 KO, alone or stably expressing mCherry tagged ARH3 WT or the chimera LANA-ARH3. The blot was stained with an ARH3 antibody. GAPDH staining was used as loading control.

SUPPLEMENTARY TABLES

Supplementary Table 1: Values of the coefficients for linear and quadratic killing estimated from the fitting of the clonogenic survival curves shown on figure 6

	WT	ARH3 KO	ARH3 OE #1	ARH3 OE #2	LANA-ARH3 #1	LANA-ARH3 #2
Linear killing term	7.1	3.1	6.2	5.9	9.6	11.9
Quadratic killing term	-4.8	-1.1	-2.2	-3.2	-5.9	-7.3

Supplementary Table 2: List of primers used in this study

Name	Sequence (5'-3')
E988K_Fwd	atgacacctctctactatataacaagtacattgtctatgatattgc
E988K_Rev	gcaatatcatagacaatgtacttgttatatagtagagaggtgtcat
mCherry_LANA _fwd	tacaagtccggactcagatctcgagggATGGCGCCCCCGGGAATG
ARH3_LANA _rev	ctgcggccatgccacctccTCTTTCCGGAGACCTGTTTCGTTTCC
LANA_ARH3_fwd	aggaggtggcATGGCCGCAGCGGCGATG
ARH3_mCherry_Rev	tcagttatctagatccggtggatccTCAACTCTTCTGGAAGACACGGTGC
ARH3_Fwd	atctcgagttATGGCCGCAGCGGCGATG
Macrodomain_Fwd	CAGGGTGAAGTCAGTAA
Macrodomain_Rev	CTAGTTGGCGTCCAGCTT
BshTI_HaloTag	aattAccggTCGCCACCatggc
Bsp1407I_HaloTag	atattgtacatggaaatctctagcgtcgacagc

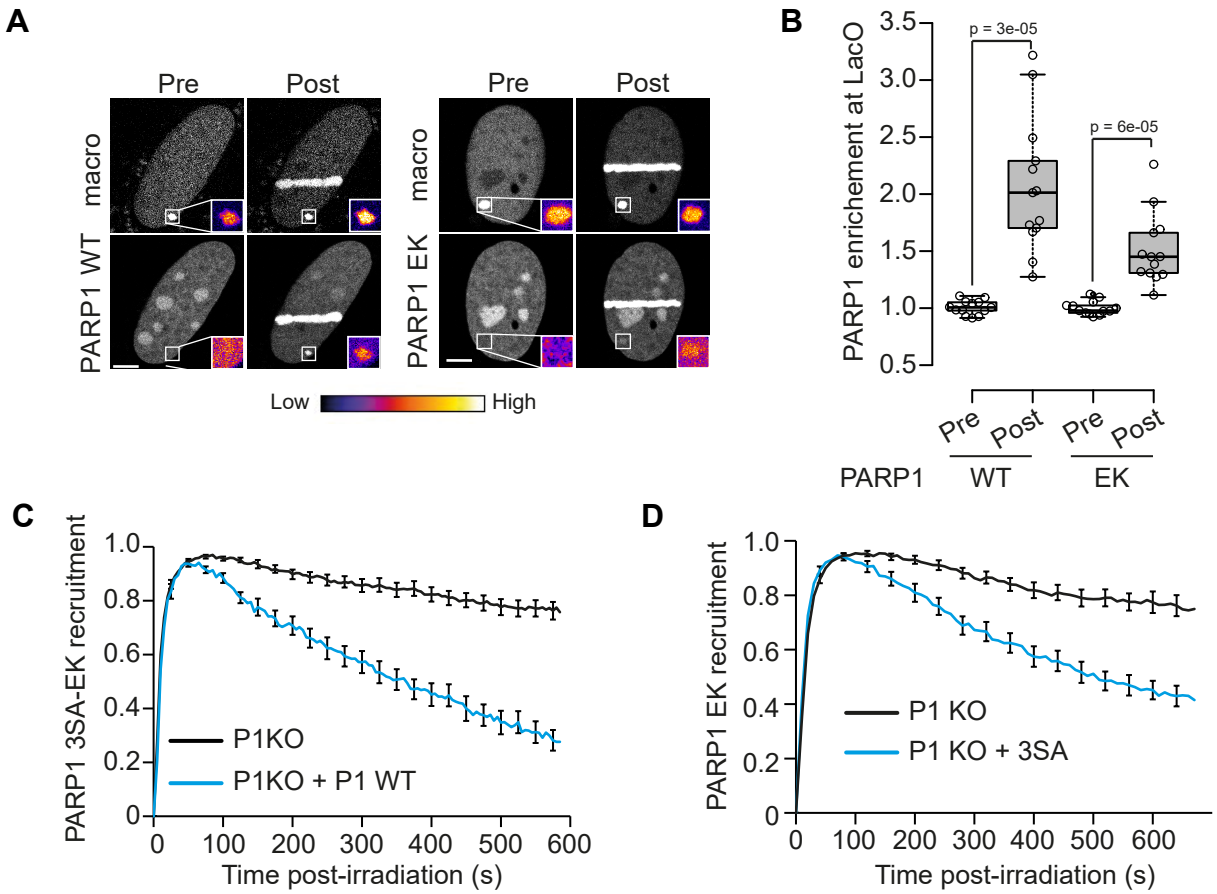

Supplementary figure 1. Heteromodification contributes to the mobilization of PARP1 from the DNA lesions. (A) Representative images of U2OS cells bearing LacO repeats and co-expressing a mCherry-tagged fusion between the LacI and the macrodomain of macroH2A1.1 and GFP tagged PARP1 WT or PARP1 E988K. Images were taken prior to damage and 50 s post irradiation with a pulsed 800 nm laser. Insets pseudocolored according to the look-up table displayed below show magnification of the LacO array. Scale bar, 5 μm. **(B)** Quantification of the PARP1 accumulation at the LacO array from the images shown in A. **(C)** Recruitment kinetics of the GFP tagged PARP1 S499/507/519A E988K (PARP1 3SA-EK) mutant after DNA damage by 405 nm laser irradiation, in PARP1 KO co-expressing or not mCherry tagged PARP1 WT. (D) Recruitment kinetics of GFP tagged PARP1 E988K after DNA damage by 405 nm laser irradiation, in PARP1 KO co-expressing or not mCherry tagged PARP1 3SA.

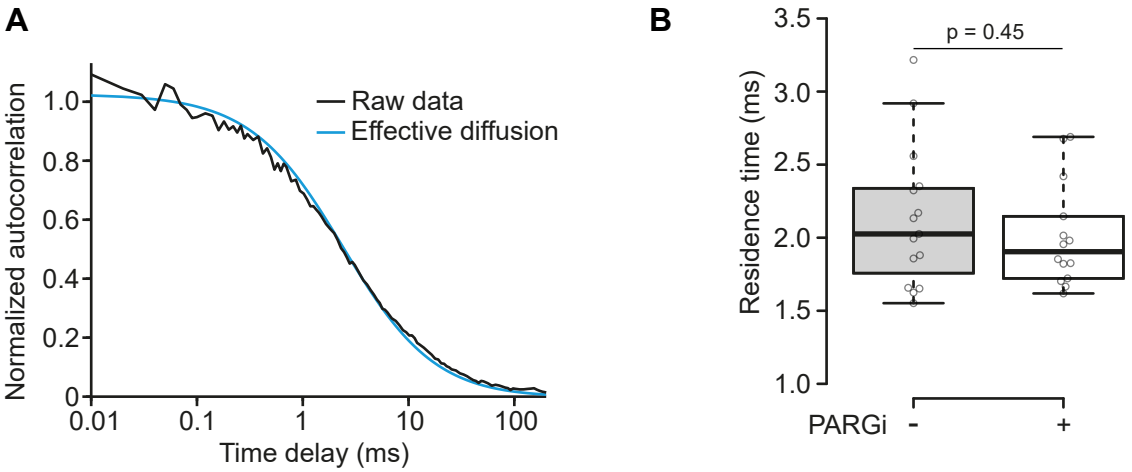

Supplementary figure 2. Impact of PARGi treatment on the nuclear dynamics of PARP1. (A) Normalized FCS correlation curve obtained for GFP tagged PARP1 WT expressed in ARH3 KO cells in the absence of PARGi treatment. The experimental curve (black line) is fitted with an effective-diffusion model (blue line). **(B)** Residence times within the focal volume estimated from the fit of the autocorrelation curves obtained for GFP tagged PARP1 WT expressed in WT cells treated or not with 20µM of the PARGi PDD00017273 for 48h.

Zentout et al., Figure S2

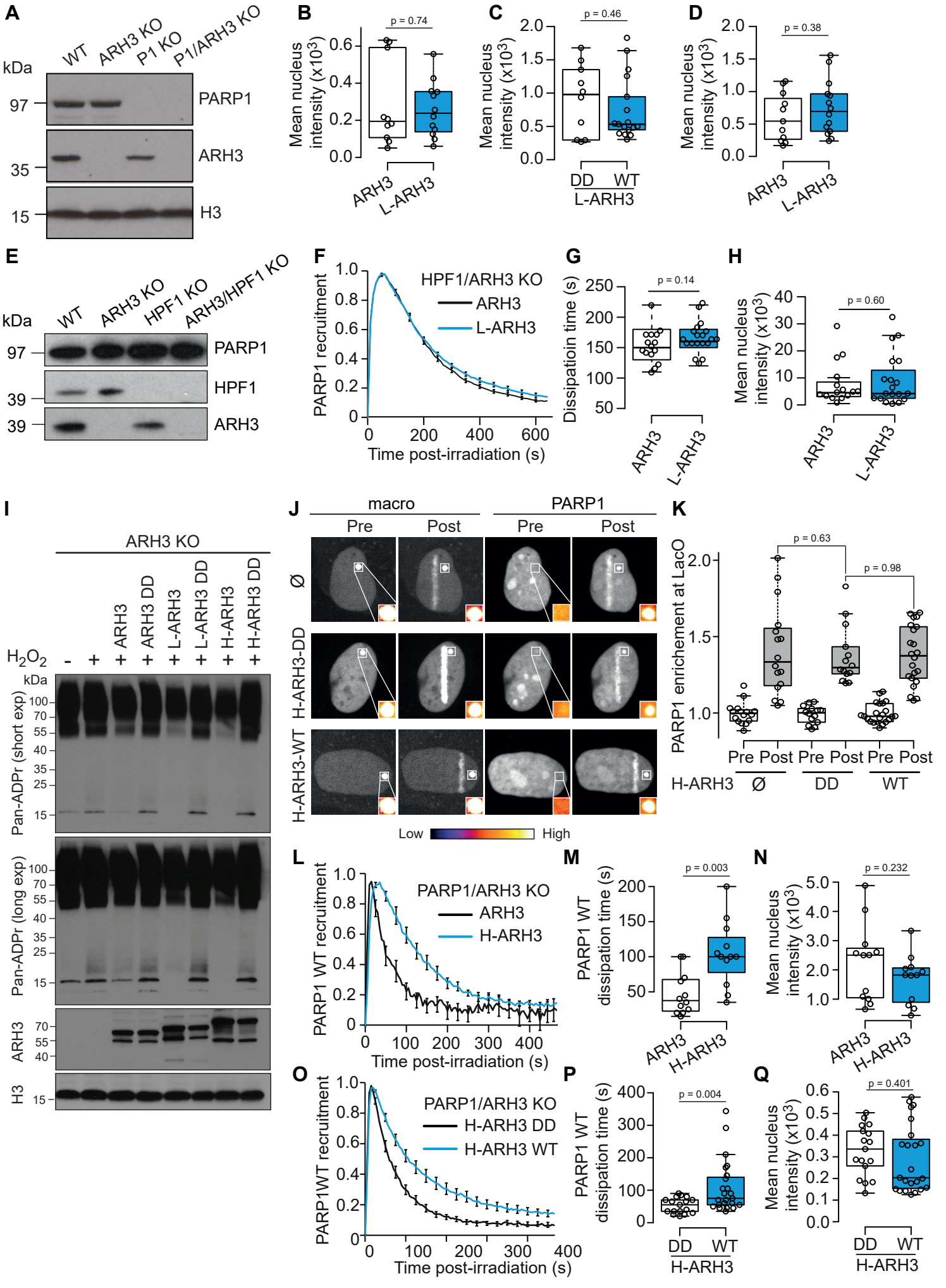

Zentout et al., Figure S3 (legend below)

Supplementary figure 3. HPF1 dependent histone ADP-ribosylation promotes PARP1 release from DNA breaks. **(A)** Immunoblot of whole-cell extract from U2OS WT, ARH3 KO, PARP1 KO and PARP1/ARH3 KO cells. The blot was stained with a PARP1 and an ARH3 antibody. H3 staining was used as loading control. **(B-D)** Mean nuclear intensities of mCherry-tagged fusion proteins as indicated. **(E)** Immunoblot of whole-cell extract from U2OS WT, ARH3 KO, HPF1 KO, and HPF1/ARH3 KO cells. The blot was stained with a HPF1 and an ARH3 antibody. PARP1 staining was used as loading control. **(F-H)** Recruitment kinetics (F), dissipation times (G) and mean nuclear intensities in the mCherry channel (H) for GFP tagged PARP1 chromobody after DNA damage by 405 nm laser irradiation, in HPF1/ARH3 KO co-expressing mCherry tagged ARH3 WT or LANA-ARH3 WT. **(I)** Immunoblot of ARH3 KO cells, untransfected, or expressing either GFP tagged ARH3 WT, ARH3 D77/78N (DD), LANA-ARH3 WT LANA-ARH3 D77/78N, H2B-ARH3 WT or H2B-ARH3 D77/78N, treated or not with H2O2. The blot was stained with a pan-ADPr and an ARH3 antibody. H3 staining was used as loading control. **(J)** Representative images of UO2S cells bearing LacO repeats and co-expressing a mCherry tagged fusion between the LacI and the macrodomain of macroH2A1.1, PARP1 WT fused to Halotag stained with JF648 and LANA-ARH3 WT or D77/78N tagged with GFP. Images were taken prior to damage and 50 s post 405 nm laser irradiation. Insets pseudocolored according to the look-up table displayed below, show magnification of the LacO array. **(K)** Quantification of PARP1 accumulation at the LacO array from the images shown in I. **(L-N)** Recruitment kinetics (L) dissipation times (M) and mean nuclear intensities in the mCherry channel (N) for GFP tagged PARP1 WT after DNA damage by 405 nm laser irradiation, in PARP1/ARH3 KO co-expressing mCherry tagged ARH3 WT or H2B-ARH3 WT. **(O-Q)** Recruitment kinetics (O), dissipation times (P) and mean nuclear intensities in the mCherry channel (Q) for GFP tagged PARP1 WT after DNA damage by 405 nm laser irradiation, in PARP1/ARH3 KO co-expressing mCherry tagged H2B-ARH3 WT or H2B-ARH3 D77/78N.

Zentout et al., Figure S3

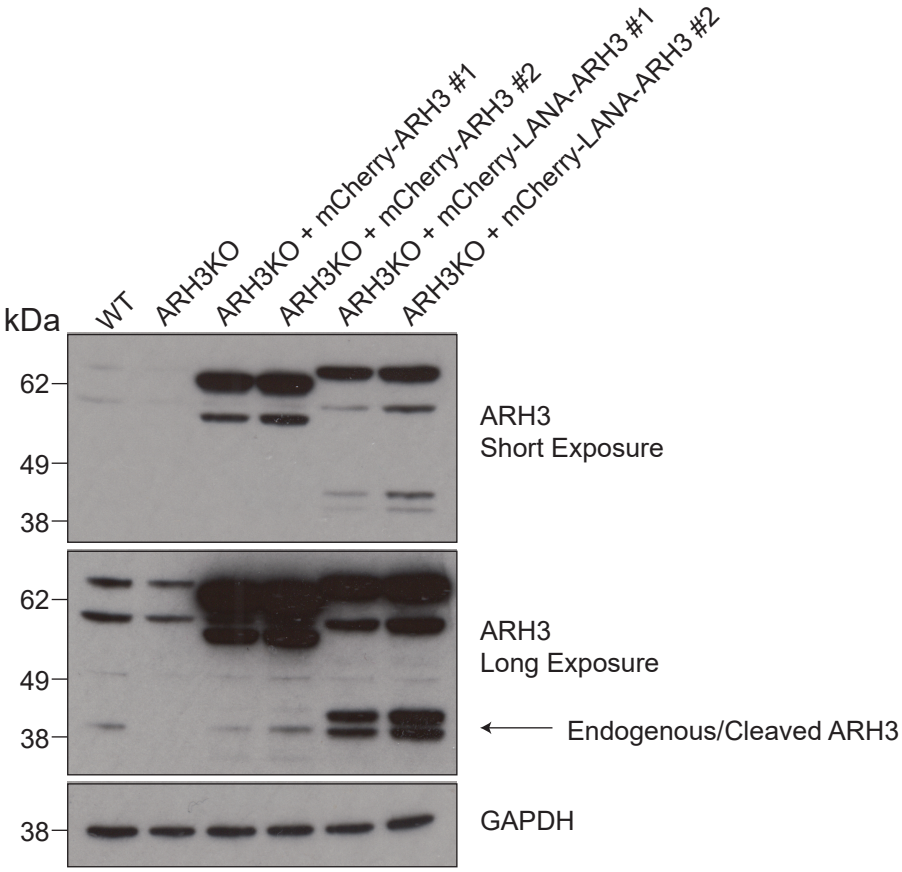

Supplementary figure 4. Histone ADP-ribosylation underlies resistance to the PARP inhibitor Olaparib. Immunoblot of whole-cell extract from U2OS WT or ARH3 KO, alone or stably expressing mCherry tagged ARH3 WT or the chimera LANA-ARH3. The blot was stained with an ARH3 antibody. GAPDH staining was used as loading control.

Zentout et al., Figure S4